



HAL
open science

A Comparative Study on the Shear Behaviour of an Interlayer Material Based on Laboratory and In-situ Shear Tests

Dingping Xu, Yu-Jun Cui, Xiating Feng, Yali Jiang, Ke Huang

► **To cite this version:**

Dingping Xu, Yu-Jun Cui, Xiating Feng, Yali Jiang, Ke Huang. A Comparative Study on the Shear Behaviour of an Interlayer Material Based on Laboratory and In-situ Shear Tests. *Geotechnical Testing Journal*, 2012, 35 (3), pp.375-386. 10.1520/GTJ103742 . hal-00700272

HAL Id: hal-00700272

<https://enpc.hal.science/hal-00700272>

Submitted on 22 May 2012

HAL is a multi-disciplinary open access archive for the deposit and dissemination of scientific research documents, whether they are published or not. The documents may come from teaching and research institutions in France or abroad, or from public or private research centers.

L'archive ouverte pluridisciplinaire **HAL**, est destinée au dépôt et à la diffusion de documents scientifiques de niveau recherche, publiés ou non, émanant des établissements d'enseignement et de recherche français ou étrangers, des laboratoires publics ou privés.

1
2 **A Comparative Study on the Shear Behaviour of an Interlayer Material Based**
3 **on Laboratory and In-situ Shear Tests**
4

5 Ding-Ping Xu¹, Xia-Ting Feng² Yu-Jun Cui^{*3}, Ya-Li Jiang⁴, Ke Huang⁵
6
7

8 ¹ Ph. D candidate, State Key Laboratory of Geomechanics and Geotechnical Engineering,
9 Institute of Rock and Soil Mechanics, Chinese Academy of Sciences, Wuhan, China 430071, E-
10 Mail: ben_johnson@163.com
11

12 ² Professor, State Key Laboratory of Geomechanics and Geotechnical Engineering, Institute of
13 Rock and Soil Mechanics, Chinese Academy of Sciences, Wuhan, China 430071, E-Mail:
14 xtfeng@whrsm.ac.cn
15

16 ^{*3} Corresponding author, Professor, UMR NAVIER/CERMES, Ecole des Ponts ParisTech, 6 et 8
17 av. Blaise Pascal, 77455 MARNE-LA-VALLEE CEDEX 2, France, E-mail: yujun.cui@enpc.fr
18

19 ⁴ Engineer, East China Investigation and Design Institute, China Hydropower Engineering
20 Consulting Group Co., Hangzhou, China 310014, E-mail: jiang_yl@ecidi.com
21

22 ⁵ Engineer, East China Investigation and Design Institute, China Hydropower Engineering
23 Consulting Group Co., Hangzhou, China 310014, E-mail: huang_k@ecidi.com
24
25
26

27 **Abstract**

28 In order to evaluate the overall stability of the underground powerhouse at the future Baihetan
29 hydropower station in China, the shear strength of a weak intercalation soil in the host rock has
30 been investigated by carrying out in-situ direct shear and laboratory shear tests. A comparative
31 study was performed based on the two testing results. It has been observed that both tests show
32 elastic perfect-plastic behaviour. A significant heterogeneity of the samples has been identified
33 under both laboratory and field conditions. The samples disturbance seems to be a factor less
34 important compared to the samples variability. The size effect has been evidenced by the greater
35 friction angle obtained in the laboratory on small samples than that obtained in the field on larger
36 samples. The clay fraction has been found to be an important factor; its increase reduces the
37 friction angle and increases the cohesion. Without considering some particular data due to the
38 soil heterogeneity, a negligible effect of initial degree of saturation has been identified.
39 Comparison between the results from the field tests with that from the laboratory tests in terms of
40 effects of the clay fraction and initial degree of saturation shows a good consistency, indicating a
41 relatively secondary effect of samples size and samples variability.

42

43 **Keywords:** Baihetan site; interlayer staggered zone; laboratory shear test; in-situ shear test;
44 shear behaviour; comparative study.

45

46 **Introduction**

47 At future Baihetan hydropower station in China, there is a weak intercalation soil in the host
48 rocks (tuff and basalt) that represents a potential threat to the overall stability of underground
49 powerhouse due to its relatively poor mechanical properties. The location of the planed
50 hydropower station is shown in Fig.1, on the downstream of Jinsha River. It is one of the largest
51 multipurpose water conservancy projects in China. In the preliminary design by the East China
52 Investigation and Design Institute (ECIDI), the hydropower station is made up of three parts, i.e.
53 the underground powerhouse, the dam and the navigation facility. The underground powerhouse
54 covers both sides of the river in the downstream direction, with the buried depths of 350 m on
55 the left bank and 550 m on the right bank. It is composed of a main powerhouse cavern, a main
56 transformation cavern and a tailrace surge tank, whose dimensions are $439 \times 32.2/29 \times 90$ m,
57 $400 \times 20.5 \times 32$ m and $311 \times 28.5/26.5 \times 88.42$ m, respectively. The horizontal distances from
58 the powerhouse area to the toes of the mountain are respectively 515 m on the left bank and
59 530 m on the right bank. Preliminary calculation shows that these distances are sufficient to
60 ensure the powerhouse stability under unloading induced by river erosion and cutting (102 m on
61 the left bank and 62 m depth on the right bank). Five slightly inclined interlayer staggered zones
62 (No.1, No.2, No.3, No.4 and No.5) with thickness ranging from 50 to 300 mm (Fig.2, in testing
63 tunnel No.62) are found in the powerhouse regions. Fig.3 shows the geological map of the
64 underground powerhouse site at an elevation of 624 m above the see level where testing tunnel
65 No.62 is located. From the figure, it can be seen that the No.4 and No.5 interlayer staggered
66 zones cross the testing tunnel at this elevation. Due to their large scope at this site the No.1, No.4
67 and No.5 interlayer staggered zones outcropped in the upper part of the high walls or arch of the
68 powerhouse.

69
70 Fig. 4 shows the grain size distribution curves of the interlayer material from the 5 zones. It can
71 be observed that the interlayer material is generally coarse-grained soils with large d_{50} values:
72 0.3 mm, 0.9 mm, 2.5 mm, 0.15 mm and 5 mm for zone No.1, No.2, No.3, No.4 and No.5,
73 respectively. In the testing tunnels, the key role of water action in the grain size of interlayer
74 material was observed: in the zones with small grain size, water flow through fractures can be
75 seen whilst in the zones with large grain size no water flow can be identified. In other words,
76 water flow enhances the formation of fine-grained soils: the more intense the water flow the
77 clayeyer the interlayer material. This explains the great difference of the physical properties
78 (water content w , unit mass ρ , specific gravity G_s , void ratio e , degree of saturation S_r , liquid
79 limit w_L , plastic limit w_P , etc.) between different interlayer materials (see Table 1). The clay
80 minerals determined by X-ray diffractometry are illite, montmorillonite, halloysite and kaolinite.

81
82 From a mechanical point of view, the shear strength of both interlayer soils and soils/rock
83 interface is much lower than the host rocks, and as a result, when excavating shear failure could
84 occur either in the soils or at the soil-rock interface. Thus the question of the stability of the
85 underground powerhouse is arisen and the shear strength behaviour of the interlayer staggered
86 zone is needed to be investigated.

87
88 The shear behaviour of interlayer staggered zone has been studied by number of researchers by
89 developing testing methods, studying the shear strength and elaborating constitutive models. Xu
90 (1980) considered the interlayer soil as a typical rheological material and observed from field
91 creep tests that the creep process was composed of three stages: decelerated creep, steady creep

92 and accelerated creep. Chen and Li (1980) observed that the relaxation of interlayer soils is an
93 important mechanism. Li et al. (1983) carried out two laboratory tests on the interlayer soil,
94 including simple shear creep test and shear stress relaxation test, to investigate its long-term
95 shear strength behaviour. Dong et al. (1994) performed field shear tests at controlled
96 displacement rate with monitoring of pore pressure and analysed the dissipation of pore pressure
97 during consolidation and shearing. Recently, the shear behaviour of completely decomposed
98 granite (CDG) soil, which is similar to the interlayer material, was studied using various test
99 apparatus and methods. For instance, Chu and Yin (2005, 2006) adopted direct shear box tests to
100 investigate the interface shear behaviour between the soil nails and CDG soil. Hossain and Yin
101 (2010) studied the shear strength and dilative characteristics of CDG soil by performing a series
102 of single-stage consolidated drained direct shear tests under different matric suctions and net
103 normal stresses. They found that the shear strength of CDG soil increases with matric suction
104 and net normal stress. The phenomenon, i.e., a greater dilation angle at higher suctions with
105 lower net normal stresses and lower or zero dilation angles under higher net normal stresses with
106 lower suctions, was observed.

107
108 As far as the creep and strength models for interlayer material are concerned, Ge (1979) and Ge
109 et al. (1982) elaborated a creep model based on the field shear test results and applied it to
110 analyse the rock displacement of the foundation pit at the site of Gezhouba dam in China. In
111 order to describe the primary, steady and accelerated creep stages under constant shear stress and
112 based on the laboratory shear tests on saturated interlayer samples, Xiao et al. (1986) proposed a
113 complex creep model made up of elastic, plastic and viscous components connected in
114 series/parallel. Regarding the shear strength, Oliveira et al. (2009) have presented a critical
115 review on the existing models for infilled materials and modified the normalised peak shear
116 stress model based on the shear tests on the idealised saw-tooth joints.

117
118 To study the shear strength behaviour of the interlayer material at Baihetan site, both in-situ
119 shear and laboratory shear tests have been carried out. This paper aims at making a comparison
120 of the results from the tests under two different conditions. This comparison is expected to be
121 helpful for better understanding the shear behaviour of the interlayer material and adopting
122 reasonable strength parameters in constitutive models.

123 124 **Materials and Methods**

125 *In-situ shear testing*

126 In-situ direct shear tests on interlayer material were carried out at the testing tunnel bottom part
127 where interlayer staggered zone is found based on the Chinese Standard SL264-2001. According
128 to this standard, in-situ sample size should be larger than $500 \text{ mm} \times 500 \text{ mm} \times h \text{ mm}$ ($h \geq 350$
129 mm). For the test by multi-sample method (MSM), 5 in-situ rock blocks in size of about 500 mm
130 $\times 500 \text{ mm} \times 350 \text{ mm}$ were carefully trimmed to prepare samples in the testing tunnel. Fig.5
131 depicts the sketch of sample for the in-situ test. For each sample, the lower part corresponds to
132 the underlying rock, and was below the ground surface; the interlayer material is at the level of
133 the ground surface and under the upper rock block. Weak or fractured rock blocks were
134 encapsulated using concrete mould and maintained under field condition for more than 14 days
135 until the strength of concrete mould achieved the testing requirement. Fig.6 shows the schematic
136 layout of the in-situ direct shear test. Before testing, normal loading system and shear loading
137 system were carefully installed in turn to ensure the resultant force to be at the centre of the

138 interlayer material. In order to guarantee the space for normal deformation, a 10-mm gap
139 between the prefixed plane and the bottom of backing plate was initially kept. When testing, a
140 prescribed normal stress σ_n was first applied and the vertical displacement was monitored using
141 displacement gauges. In order to avoid the extrusion of interlayer material especially at high
142 initial degree of saturation, as discussed by Sun and Zhao (1980), a normal stress lower than 1.5
143 MPa was applied in 4 steps of 5-min duration. Equilibrium was considered as reached when the
144 displacement rate is lower than 0.03 mm/10 min. Shear stress τ was then applied under constant
145 normal stress until the sample reached failure or the shear displacement (u_s) was larger than 15
146 mm along the prefixed plane. A total of 8 - 12 shear loading steps of 10 min each were
147 considered. This procedure was repeated when testing other samples at different values of σ_n .
148 The results allowed the determination of the strength parameters. As shown in Table 2, the
149 degrees of saturation of the samples were high, from 73.0% to 99.5%.

150

151 *Laboratory shear testing*

152 Two laboratory shear tests were performed, including the direct shear test using the shear system
153 RMT150C (Fig.7) and the shear creep tests using the system JQ-200 (Fig.8). When conducting
154 direct shear test on RMT150C, normal stress was applied through an adjustable vertical piston
155 and shear was applied through a horizontal loading system that drives two horizontal dowels
156 pushing the upper shear box. The dimensions of the samples for these tests were 150 mm \times 150
157 mm \times 150 mm, with the interlayer material in the middle and the concrete blocks at both the top
158 and bottom (see in Fig.7 and Fig.8). In the sample, the block interlayer was taken from a block
159 with a dimension of 180 mm \times 180 mm \times h mm (h was the thickness of interlayer material).
160 Note that the interlayer blocks were dug from testing tunnel No.41 (near the left bank
161 powerhouse region whose depth is 350 m) and testing tunnel No.62 (in the right bank
162 powerhouse region whose depth is 550 m). Before preparing laboratory shear test samples, the
163 block interlayer material was first cut carefully into a sub-block of 150 mm \times 150 mm \times t mm (t
164 was the thickness of interlayer material, $t \leq h$). After that, the sample was prepared using a metal
165 mould without upper and lower covers, as follows: pouring the concrete with the quantity needed
166 to reach the lower concrete height calculated previously according to the thickness of interlayer
167 material; putting the sub-block on the lower concrete; pouring the upper concrete with the
168 quantity needed to reach the upper concrete height calculated previously; disassembling the
169 metal mould and conserving the sample in a vertical position under indoor condition. Note that
170 the thickness t was in general more than 30 mm, enough to ensure the shear failure to occur in it.
171 In order to analyze the effect of initial degree of saturation, laboratory direct shear tests were
172 conducted at much lower degree of saturation (see Table 3 and Table 4, ranging from 17.9% to
173 48.7%) than that in field (ranging from 73% to 99.5%). However, Greater values of degree of
174 saturation were considered in the laboratory when investigating its effect on the creep behaviour.

175

176 Two methods, i.e. MSM for direct shear testing and Single-sample method (SSM, see Zhang et
177 al., 1994) for direct shear and shear creep testing, were adopted. For direct shear test by MSM,
178 the procedure is similar to the in-situ direct tests described above. For direct shear test by SSM,
179 normal stress and shear stress were step loaded alternatively. In the first step loading, normal
180 stress was applied in 4 steps of 5-min duration each. When peak point or constant τ was observed
181 on τ - u_s curve during a step loading, the next step σ_n and τ are applied. By varying σ_n and τ more
182 than 4 times before the sample failure, the τ - σ_n plot can be drawn and then shear strength
183 parameters can be determined. For shear creep test by SSM, the procedure follows the Chinese

184 Industry Standard SL264-2001: shear stress was applied in more than 5 steps on a sample under
185 a prescribed normal stress, with each loading step kept for longer than 5 days. Note that the
186 sample area correction was applied for direct shear tests when calculating the stress values, and
187 as a result, the normal stress before the first shear loading by MSM corresponds to the initial
188 normal stress and the τ - u_s curves seem to increase even after failure.
189

190 **Experimental results**

191 *In-situ tests*

192 Fig.9a shows the τ - u_s curve from the test in zone 1 on the interlayer material at a degree of
193 saturation of 76.6%. Note that due to a technique problem, the vertical deformation was not
194 available. It can be observed from the figure that i) only the test under a normal stress of
195 1.05 MPa depicts a peak shear stress, other tests showing a plateau of stabilisation; ii) only the
196 increase of the maximum shear stress when increasing the normal stress from 0.34 MPa to 0.46
197 MPa is significant, the values for other tests are close. Normally, for a given soil with increasing
198 normal stress, the shear stress peak is less pronounced and the increase of maximum shear stress
199 is proportional to the normal stress increase. The observations made on this test are to be
200 attributed to the variability of the five test samples. Fig.9b depicts the results from the tests in
201 zone 2 at an initial degree of saturation of 73.0%. Only the test under 0.98 MPa normal stress
202 shows an apparent peak, other tests giving a plateau of stabilisation. The increase of maximum
203 shear stress with increasing normal stress is more regular than the tests in zone 1, indicating a
204 less pronounced variability of the tested samples. Fig.9c depicts the results from the tests in zone
205 3 at an initial degree of saturation of 96.6%. No peaks are observed and all tests show a plateau
206 of stabilisation. The increase of shear stress with increasing normal stress is also relatively
207 regular, indicating that the samples tested are relatively similar. The test under 1.26 MPa normal
208 stress shows a singular shape, with a sudden decrease of slope at about 0.40 MPa shear stress
209 followed by an increase from 0.45 MPa shear stress. This phenomenon is suspected to be ‘pores
210 collapse’ or ‘grains crushing’. Further study is needed to investigate this fundamental
211 phenomenon. Fig.9d depicts the results from the tests in zone 4 at an initial degree of saturation
212 of 93.5%. Only the test under 1.02 MPa normal stress shows a singular behaviour with a shear
213 stress continuously increasing, even exceeding the maximum value under a higher normal stress
214 (1.26 MPa). Visual Examination of the tested sample confirms this observation; indeed, this
215 sample shows an irregular shear surface with two parts of a difference of 30 mm in height (see
216 Fig.10). Fig.9e depicts the results from the tests in zone 5 at an initial degree of saturation of
217 76.6%. Normal behaviour can be observed: the shear stress increases regularly with increasing
218 normal stress, showing a low variability between the tested samples.
219

220 The cohesion c and friction angle φ were determined based on the obtained τ - u_s curves, and are
221 presented in Table 2. The results show a quite large scatter: the values of c range from 0.02 to
222 0.42 MPa and the values of φ ranges from 14° to 38°. This large scatter can be attributed to the
223 effects of degree of saturation (ranging from 73.0% to 99.5%) and the clay fraction (ranging
224 from 0 to 13.0%); it can be also attributed to the heterogeneity of the samples as observed above.
225

226 *Laboratory tests*

227 Fig. 11 shows the results obtained from laboratory shear tests by MSM on the interlayer material
228 from testing tunnel No.62 with the initial degree of saturation between 17.9% and 48.7%, under
229 different normal stresses: 2.0 MPa, 3.0 MPa, 4.0 MPa and 5.0 MPa. Note that a step-loading

230 procedure was applied in these tests; this explains the observed shapes of the curves. The τ - u_s
231 curves show identical behaviour when the shear stress is lower than 1.5 MPa, indicating, to a
232 certain extent, a similar elastic behaviour. Beyond 1.5 MPa shear stress, the shear stress is higher
233 with a higher normal stress. The u_n - u_s curves (u_n is the vertical displacement) do not show any
234 shear dilatancy: the volume change is compressive for all the tests conducted. Similar behaviour
235 is observed for $u_n < 0.5$ mm. Interestingly, this range corresponds to the range of $\tau < 1.5$ MPa
236 identified above on the τ - u_s curves. Examination of the u_n - u_s curves corresponding to 2.0 and 3.0
237 MPa normal stress shows that the material is more compressive under higher normal stress; this
238 is normal behaviour generally observed on other soils. A problem can be identified on the curves
239 of 4.0 MPa and 5.0 MPa normal stress: the curve of $\sigma_n = 4.0$ MPa shows much larger
240 compression than that of $\sigma_n = 5.0$ MPa. This can be attributed to the heterogeneity of the soil
241 samples. Based on the τ - u_s curves obtained, the values of σ_n and τ_p at failure are determined and
242 presented in Table 3. Fig.12 depicts the values of σ_n and τ_p at failure from all the tests by MSM.
243 It can be observed that it is difficult to obtain reasonable shear strength parameters due to the
244 significant scatter of data.

245 Fig. 13 shows a typical result from the shear test by SSM on the interlayer material taken from
246 testing tunnel No. 62 at an initial degree of saturation of 33.1%. A total of 7 loading steps were
247 applied. It can be observed from the τ - u_s curve that stabilisation was reached for each loading
248 step. Examination of the u_s - u_n curve shows that for most loading step the vertical displacement
249 shows a quasi-immediate drop followed by a variation with a smaller slope. The shear strength
250 parameters determined from the test results are presented in Table 4.
251

252 Fig. 13 depicts the creep behaviour in the u_s - t plane (t is the time) under a normal stress $\sigma_n =$
253 0.49 MPa and at various shear stresses: 0.09 MPa, 0.18 MPa, 0.27 MPa, 0.37 MPa, 0.46 MPa,
254 0.55 MPa, 0.64 MPa and 0.74 MPa. It can be observed that the creep is not significant: under
255 different shear stresses, the u_s - t curves show that most deformation occurs within a short time
256 and the creep deformation is negligible. This differs from the previous studies in which interlayer
257 material was considered as a rheological material (Xu 1980; Li and Kang 1983; Xiao 1987).
258 From a practical point of view, this observation is of importance because relatively simple
259 elastoplastic constitutive models can be used to describe the behaviour of interlayer material and
260 there is no need to pay special attention to its creep behaviour. Moreover, the results from the
261 creep tests can be used to determine the strength parameters.
262

263 It is to be noted that in the direct shear test, it is an important issue as to keep uniform vertical
264 pressure on soil sample during shearing. Bathurst et al. (2008) carried out direct shear tests with
265 three different loading methods for vertical stress, using: (1) a flexible airbag, (2) a fixed vertical
266 piston, and (3) an adjustable vertical piston. They found that 1) the non uniform vertical stress
267 distribution occurs when the soil shows shear dilatancy, almost uniform vertical stress being
268 observed in all cases. and (2) the best method for keeping uniform vertical stress is the flexible
269 airbag method. In this study, the method of adjustable piston method was employed, and in
270 addition no dilatancy was observed during shearing (see Fig.11 and Fig.13). Thus, it is supposed
271 that this phenomenon of non uniform vertical stress distribution was not significant in the present
272 work.
273

274 **Comparative analysis based on in-situ and laboratory measurements**

275

276 Both in-situ and laboratory shear tests were carried out on the interlayer material. This allows a
277 comparison between the results obtained under the two test conditions. This comparison can be
278 done in terms of the effects of soil heterogeneity, sampling disturbance, sample size, clay
279 fraction and initial degree of saturation. Because the vertical displacement was not obtained from
280 the in-situ tests for technical problems, the study was limited to the comparison of the strength
281 parameters: c and φ . In addition, due to the difficulty of determining the strength parameters
282 based on the results from the laboratory shear tests by MSM (see Fig.12), a special procedure of
283 data treatment was then applied, as follows:

- 284 1) to attribute a relatively large value of 0.2 MPa to c based on the values from both
285 laboratory direct shear tests by SSM and in-situ shear tests,
- 286 2) to back calculate φ value based on the data according to the Mohr-Coulomb criterion
287 (Eq. 1):

$$288 \tau = c + \sigma_n \tan \varphi \quad (1)$$

289 The calculated values are presented in Table.3. It can be observed that relatively large values of
290 friction angle were obtained, between 20.5° and 38.7° . Note that the φ values obtained from this
291 special procedure of data treatment were not used to analyze the effects of clay fraction and
292 initial degree of saturation.

293

294 *Effects of soil heterogeneity and sampling disturbance*

295 Soil heterogeneity is a common problem when dealing with intact natural materials. For the in-
296 situ tests, the heterogeneity caused significant data scatter and rendered the determination of
297 strength parameters difficult (zone 1, see Fig. 9a). Some samples from the same zone showed
298 different specific phenomenon as the suspected pores collapse or grains crushing (zone 3, see Fig.
299 9c). The difference between the samples from different sampling zone is quite large: the
300 maximum shear stress value is about 0.50 MPa for zone 1 ($\sigma_n = 1.05$ MPa), 1.70 MPa for zone 2
301 ($\sigma_n = 1.26$ MPa), 0.75 MPa for zone 3 ($\sigma_n = 1.26$ MPa), 0.36 MPa for zone 4 ($\sigma_n = 1.26$ MPa),
302 and 0.90 MPa for zone 5 ($\sigma_n = 1.41$ MPa). As far as the laboratory tests are concerned, the results
303 from MSM tests have depicted such a significant variability that the determination of shear
304 parameters using the common results was not possible. The SSM method was then applied for
305 this purpose. The results obtained have shown that this method is efficient and probably the only
306 method allowing the direct determination of the shear strength parameters of the interlayer
307 material.

308

309 Because both in-situ tests and laboratory tests involve the problem of sample disturbance, the
310 samples do not reflect the real soil behaviour totally. Moreover, it is believed that this sample
311 disturbance is more significant for the laboratory testing samples because (1)) the soil blocks are
312 taken by removing the material in all directions, one direction more that the sample for in-situ
313 testing; (2) there were transportation and conservation for the laboratory samples; (3) extra
314 trimming was applied when preparing the laboratory samples. In spite of the unavoidable sample
315 disturbance, as significant variability was observed when testing the interlayer material under
316 both field and laboratory conditions, it seems that the problem related to the sample disturbance
317 is not an important factor compared to the samples variability due to the material heterogeneity.

318

319 *Effects of sample size*

320 The shear plane for the laboratory samples is 150×150 mm while the rock particles can reach a
321 diameter of 100 mm (see Fig 4). The dimension and the proportion of these large rock particles

322 in the soil matrix can play an important role in the shear strength determined, as reported by
323 several authors (Holtz and Gibbs 1956; Dobbiah et al. 1969; Iannacchione and Vallejo 2000;
324 Vallejo and Mawby 2000; Cerato and Lutenegeger 2006; Fakhimi and Hosseinpour 2008). Holtz
325 et al. (1956) showed that there is a critical fraction of coarse rock particles (35%) that affect the
326 shear behaviour of soil-rock mixture. Dobbiah et al. (1969) confirmed this observation but found
327 a value of 50% for the critical fraction; this indicates that this value is dependent on the nature of
328 the soil matrix and the coarse particles. If the fraction of rock particles is beyond this value, the
329 shear strength is dominated by the particle-to-particle contacts. According to the China National
330 Standards GB/T 50145-2007, the particle diameter of 0.075 mm is the border between fine-
331 grained particles and coarse particles. Following this definition, one can identify the coarse rock
332 particles of the interlayer material based on the grain size distribution curves shown in Fig.4:
333 71% for zone 1; 77% for zone 2; 82% for zone 3; 59% for zone 4; 87% for zone 5. Thus, all
334 values are beyond the critical fraction. As a result, the behaviour must be dominated by coarse
335 particles. Note however that as a natural soil, the interlayer material is significantly different
336 from the artificially prepared soil-rock mixtures in which rock particles are uniformly distributed
337 in soil matrix. With a randomly distributed rock particles in the sample, the effect of sample size
338 must be greater: the determined strength parameters, especially the friction angle are in general
339 larger in the case of small samples. It is indeed the case when comparing the friction angle
340 obtained in the laboratory by MSM and SSM with that obtained in the field (see Table 3 and
341 Table 4).

342
343 As the difference between the values of friction angle by MSM and SSM is concerned, as
344 described above, a relatively large value of cohesion (0.2 MPa) was taken when estimated the
345 friction angle based on the data from the laboratory direct shear tests by MSM. Note that this is
346 justified by the fact that most values of cohesion from both laboratory direct shear tests by SSM
347 and in-situ shear tests are smaller than 0.15 MPa (see Table 2 and Table 4). In spite of this, the
348 values obtained are in general greater than that from the laboratory direct shear tests by SSM (see
349 Table 4), indicating that the MSM gives rise to greater friction angle values than the SSM. The
350 same observation was made by other researchers on soft rock (Liu 1988; Zhang 1994). It has
351 been concluded that for the same sample, because of cumulative damage during step loadings in
352 the test by SSM, the shear strength is slightly lower than that from the tests by MSM.

353 354 *Effect of clay fraction*

355 Fig. 15a depicts the variation of friction angle with the clay fraction, under both the laboratory
356 and field conditions. The values of initial void ratio and degree of saturation of some 'points' are
357 indicated. A large variation of clay fraction can be observed, from 0 to 13%, indicating a large
358 heterogeneity of the samples. As a whole, the friction angle is decreasing with the increase of
359 clay fraction (without considering some particular points); this is logical because fine-grained
360 soils have relatively smaller friction angles than coarse soils. The values obtained from the
361 laboratory tests are consistent with that obtained from the in-situ tests. This seems to show that
362 the size effect discussed above is not so important compared with the clay fraction effect.

363
364 Fig. 15b shows the variation of cohesion with the clay fraction, under both laboratory and field
365 conditions. Some singular points are identified and the corresponding values of initial void ratio
366 and degree of saturation are indicated in the figure. Despite the significant scatter of the data, an
367 increase trend with clay fraction increase can be identified (without accounting for the particular

368 data). This is also logical when considering its role of glue in the interlayer material. The values
369 obtained from the laboratory tests are in general consistent with that from the field tests,
370 indicating again a relatively less important sample size effect.

371

372 *Effect of initial degree of saturation*

373 It is well known that the shear strength of unsaturated soils is suction or degree of saturation
374 dependent: the shear strength increases with suction increase (see for instance Fredlund et al.
375 1978; Fredlund and Rahardjo 1993). Delage and Cui (2001) analysed the data in the literature
376 and found that the cohesion always increases with suction increase, whatever the soil nature.
377 However, the friction angle can decrease or increase with suction increase, depending on the soil
378 nature and the soil density: for clayey soils, no decrease can occur (Escario and Saez 1986); on
379 the contrary for sandy soils (Escario and Saez 1986) and compacted silty soil (Maâtouk et al.
380 1995), a decrease can take place when the density is low (collapsible structure), and a slight
381 increase can take place when the density is high (Delage and Cui 2001).

382

383 For the studied interlayer material, as shown in Table 1, the clay fraction is small and the density
384 is quite high. Thus logically no friction angle decrease and a slight cohesion increase should be
385 observed with suction increase or degree of saturation decrease. Fig.16a and Fig.16b depict the
386 variation of friction angle and cohesion with the initial degree of saturation, respectively. The
387 values of initial void ratio and clay fraction of some particular 'points' are indicated in the
388 figures. Despite the significant data scatter, a negligible effect of initial degree of saturation can
389 be identified, if the particular data were excluded. A good consistency can be also observed
390 when comparing the results from the field tests with that from the laboratory tests, indicating
391 again the relatively low effect of samples size.

392

393 **Conclusions**

394

395 In order to analyse the stability of the underground powerhouse at the future Baihetan
396 hydropower station in China, the shear strength of the involved interlayer material has been
397 investigated by carrying out both in-situ and laboratory shear tests. A comparative study was
398 done in order to assess the effects of different factors as the heterogeneity, the samples
399 disturbance, the samples size, the clay fraction and the initial degree of saturation. The following
400 conclusions can be drawn:

- 401 1) the significant heterogeneity of the samples caused significant data scatter and rendered
402 the determination of strength parameters difficult; it seems that the samples disturbance is
403 not an important factor compared to the samples variability;
- 404 2) the samples are characterised by a randomly distributed coarse rock particles; this
405 explains the greater friction angle obtained in the laboratory than that obtained in the field;
- 406 3) the friction angle is an important factor affecting the shear strength: the friction angle
407 seems to decrease and the cohesion tends to increase with the increase of clay fraction;
- 408 4) without considering some particular data, a negligible effect of initial degree of saturation
409 has been identified;
- 410 5) a good consistency has been observed when comparing the results from the field tests
411 with that from the laboratory tests in terms of variations of friction angle and cohesion
412 with the clay fraction and the initial degree of saturation, evidencing that the effects of

413 samples size and samples variability are less important when compared with the effect of
414 clay fraction, or to a less extent the initial degree of saturation.

415
416

417 **Acknowledgement**

418 The work is supported by National Special Funds of China for Major State Basic Research
419 Project under Grant No. 2010CB732006, and by Chinese Academy of Sciences and State
420 Administration of Foreign Experts Affairs, P.R of China, for the CAS/SAFEA International
421 Partnership Program for Creative Research Teams under Grant No. KZCX2-YW-T12. The
422 authors are grateful to ECIDI for providing the field test data.

423

424 **NOTATIONS:**

425

c	cohesion
e	void ratio
G_s	specific gravity
h	the thickness of interlayer staggered zone in field
S_r	degree of saturation
t	the thickness of interlayer material obtained from testing tunnels
u_s	horizontal displacement
u_n	vertical displacement
w	water content
w_L	liquid limit
w_P	plastic limit
ρ	unit mass
σ_n	normal stress
τ	shear stress
τ_p	peak shear stress
ϕ	friction angle

426

427 **References**

- 428 [1] Bathurst, R. J., Althoff, S., and Linnenbaum, P., 2008, "Influence of test method on
429 direct shear behavior of segmental retaining wall units," *Geotech. Test. J.*, Vol. 31, No.
430 2, pp. 1–9.
- 431 [2] Cerato, A.B., and Lutenecker, A.J., 2006, "Specimen size and scale effects of direct
432 shear box tests of sands," *Geotech. Test. J.*, Vol. 29, No. 6, pp. 507-516.
- 433 [3] Chen, Z. J.(Tan Tjong Kie), and Li, K. R., 1981, "Relaxation and creep properties of
434 thin interbedded clayey seams and their fundamental role in the stability of dams,"
435 *Proceedings of the International Symposium on Weak Rock*, Tokyo, Japan, pp. 369–374.
- 436 [4] Chu, L. M., and Yin, J. H., 2005, "Comparison of Interface Shear Strength of Soil Nails
437 Measured by both Direct Shear Box Tests and Pull-out Tests," *J. Geotech. Geoenviron.*
438 *Eng.*, Vol.131, No.9, pp.1097-1107.
- 439 [5] Chu, L. M., and Yin, J. H., 2006, "Study on Soil-Cement Grout Interface Shear
440 Strength of Soil Nailing by Direct Shear Box Testing Method," *Geomech. Geoeng.: An*
441 *Int. J.*, Vol. 1, No.4 , pp. 259-273.
- 442 [6] Delage, P., and Cui, Y. J., 2001, "Comportement mécanique des sols non saturés,"
443 *Technique de l'Ingénieur*, C302.

- 444 [7] Dobbiah, D., Bhat, H. S., and Somasekhar, P. V., 1969, "Shear characteristics of soil-
445 gravel mixtures," *J. India Nat. Soc. Soil Mech. Found. Eng.*, No. 8, pp. 57-66.
- 446 [8] Dong, Z. D., and Yuan, C. W., 1994, "Researches For Controlled Displacement-Rate
447 Shear Test In Situ in Rock Mass Soft Intercalation," *Chin. J. Rock Mech. Eng.*, Vol.16,
448 No. 6, pp. 21-29.
- 449 [9] East China Investigation and Design Institute, 2006, "Engineering geology report for
450 dam site selection of Baihetan hydropower station at feasibility study stage," Hangzhou,
451 in Chinese.
- 452 [10] East China Investigation and Design Institute, 2008, "Preliminary design scheme of
453 underground powerhouse at Baihetan hydropower station," Hangzhou, in Chinese.
- 454 [11] Escario V., and Saez J. 1986, "The shear strength of partly saturated soils,"
455 *Géotechnique* **36** (3), pp.453-456.
- 456 [12] Fakhimi, A., and Hosseinpour, H., 2008, "The role of oversize particles on the shear
457 strength and deformational behavior of rock pile material," ARMA08-204, *The 42nd*
458 *US Rock Mechanics Symposium and 2nd US-Canada Rock Mechanics Symposium*, San
459 Francisco, USA.
- 460 [13] Fredlund, D. G., and Rahardjo, H., 1993, "Soil Mechanics for Unsaturated Soils," John
461 Wiley and Sons, Inc. New York, N.Y.
- 462 [14] Fredlund, D. G., Morgenstern, N. R., and Widger, R.A., 1978, "The Shear Strength of
463 Unsaturated Soils," *Can. Geotech. J.*, Vol. 15, No. 3, pp. 313-321.
- 464 [15] Ge, X. R. (Ke Hsu Jun), 1979, "Non-linear Analysis of the Mechanical Properties of
465 Joint and Weak Intercalation in Rock," *Proceedings of the 3rd International*
466 *Conference on Numerical Methods in Geomechanics*, Aachen, Germany, Vol. 2, pp. 2-
467 6.
- 468 [16] Ge, X. R., Feng, D. X., and Yang, J. L., 1982, "The Elasto-Visco-Plastic Analysis for
469 Rock Displacement of the Foundation Pit of a Water Hydropower Plant," *Rock Mech.*
470 *Rock Eng.*, Vol. 15, No. 3, pp. 145-161.
- 471 [17] Holtz, W. G., and Gibbs, H. J., 1956, "Triaxial shear tests on pervious gravelly soils,"
472 *J. Soil Mech. Found. Div. ASCE*, Vol. 82, No.1, pp. 1-22.
- 473 [18] Hossain, M. A., and Yin, J. H., 2010, "Shear strength and dilative characteristics of an
474 unsaturated compacted completely decomposed granite soil," *Can. Geotech. J.*, Vol.47,
475 No.10, pp. 1112-1126.
- 476 [19] Iannacchione, A. T., and Vallejo, L. E., "Shear Strength Evaluation of Clay-Rock
477 Mixtures," *Slope Stability 2000, Proceedings of Sessions of Geo-Denver 2000 Denver*,
478 Colorado, August 5-8, Geotechnical Special Publication No. 101, Editors; Griffiths D.
479 V., Fenton G. A. and Martin T. R., Reston, VA: American Society of Civil Engineers,
480 pp. 209-223.
- 481 [20] Li, K. R., and Kang, W. F., 1983, "Creep Testing of Thin Interbedded Clayey Seams in
482 Rock and Determination of Their Long-term Strength," *Chin. J. Rock Soil Mech.*, Vol.
483 4, No. 1, pp. 39-46.
- 484 [21] Liu, X., 1990, "A Study of Single Specimen Test Method for Determination of Shear
485 Strength of Softrock," *Chin. J. Rock Mech. Eng.*, Vol.9, No. 1, pp. 63-67.
- 486 [22] Maâtouk A., Leroueil S., and La Rochelle P. 1995, "Yielding and critical state of a
487 collapsible unsaturated silty soil," *Géotechnique* **45** (3), 465-477.

- 488 [23] Oliveira, D. A. F., Indraratna, B., and Nemcika, J., 2009, "Critical review on shear
489 strength models for soil-infilled joints," *Geomech. Geoeng.: An Int. J.*, Vol. 4, No.3, pp.
490 237-244.
- 491 [24] Sun, G. Z., and Zhao, R. H., 1984, "Normal stress for the shear test on weak
492 intercalation," *Chin. J. Hydrogeol. Eng. Geol.*, No.4, pp: 32-34.
- 493 [25] The Ministry of Water Resources of China, 2001, "China Industry Standards SL264-
494 2001: Specifications for Rock Tests in Water Conservancy and Hydroelectric
495 Engineering," China Water Hydropower Press, Beijing.
- 496 [26] The Ministry of Water Resources of China, 2007, "China National Standards GB/T
497 50145-2007: Standard for engineering classification of soil," China Planning Press,
498 Beijing.
- 499 [27] The Standardization Administration of China, the Ministry of Construction of China,
500 and the Ministry of Water Resources of China, 1999, "China National Standards
501 GB/T50123-1999: Standard for soil test method," China Planning Press, Beijing.
- 502 [28] Vallejo, L. E., and Mawby, R., 2000, "Porosity influence on the shear strength of
503 granular material-clay mixtures," *Eng. Geol.*, Vol. 58, No. 2, pp. 125-136.
- 504 [29] Xiao, S. F., Wang, X. F., and Chen Z. F., et al., 1986, "The Creep Model of the
505 Intercalated Clay Layers and the Change of their Microstructure during Creep,"
506 *Proceedings 5th International Congress International Association of Engineering
507 Geology*, Buenos Aires, Argentina, Vol. 4, pp. 2185-2192.
- 508 [30] Xu, D. J., 1980, "The Rheological Behaviour of the Weak Rock Mass and the Method
509 of Determining Long-Term Strength," *Chin. J. Rock Soil Mech.*, Vol. 2, No. 1, pp. 37-
510 50.
- 511 [31] Zhang, J. D., Liu, P. T., and Huang, C. J., 1994, "Mechanism for Shear Failure of
512 Weak Structural Plane and Fissured Rock," *Chin. J. Geotech. Eng.*, Vol. 16, No. 6, pp.
513 21-29.

List of Tables

Table 1 Physical properties of interlayer material (ECIDI 2006)

Table.2 Initial parameters of the samples and strength parameters for the in-situ tests

Table.3 Initial parameters of the samples and strength parameters for the laboratory tests by MSM

Table.4 Initial parameters of the samples and strength parameters for the laboratory tests by SSM

List of Figures

Fig.1. Location of Baihetan hydropower station.

Fig.2. Interlayer staggered zone in testing tunnel No.41.

Fig.3. Geological map at an elevation of 624 m where testing tunnel No.62 is located (1) $P_2\beta_2^3$: Aphanitic basalt, amygdaloidal basalt, breccia lava; (2) $P_2\beta_3^1$: Aphanitic basalt, breccia lava with oblique basalt and amygdaloidal basalt with oblique basalt; (3) $P_2\beta_3^{2-1}$: Amygdaloidal basalt; (4) $P_2\beta_3^{2-2}$: Columnar jointed basalt; (5) $P_2\beta_3^{2-3}$: Breccia lava; (6) $P_2\beta_3^3$: Columnar jointed basalt; (7) $P_2\beta_3^4$: Amygdaloidal basalt, aphanitic basalt and breccia lava; (8) $P_2\beta_3^5$: Oblique basalt, breccia lava; (9) $P_2\beta_4^1$: Columnar jointed basalt, amygdaloidal basalt, breccia lava and microcrystalline basalt; (10) $P_2\beta_4^2$: Amygdaloidal basalt, breccia lava; (11) $P_2\beta_5^1$: Aphanitic basalt and amygdaloidal basalt; (12) $P_2\beta_6^1$: Columnar jointed basalt and breccia lava; (13) $P_2\beta_6^2$: Aphanitic basalt and breccia lava; (14) Q_4^{col+dl} : Quaternary unconsolidated deposits.

Fig.4. Grain size distribution of interlayer material.

Fig. 4. Particle Grain size distribution of interlayer material.

Fig. 5. The sketch of sample for the in-situ direct shear test

Fig.6. Schematic layout of in-situ direct shear test.

Fig.7. Schematic diagram of RMT150C.

Fig.8. Schematic diagram of JQ-200.

Fig.9. Typical results of interlayer materials of in-situ direct shear tests where the size of sample is 500 mm × 500 mm × 350 mm: from the interlayer staggered zone No.1 at an initial degree of saturation $S_r = 76.6\%$ (a), from the interlayer staggered zone No.2 at an initial $S_r = 73.0\%$ (b), from the interlayer staggered zone No.3 at an initial $S_r = 96.6\%$ (c), from the interlayer staggered zone No.4 at an initial $S_r = 93.5\%$ (d), and from the interlayer staggered zone No.5 at an initial $S_r = 76.6\%$ (e).

Fig.10. The shear surfaces of samples for a set of in-situ shear tests in zone 4: (a) normal shear surface, (b) irregular shear surface. The unit of numbers is centimeter, the negative number means the region is below the prefix shear plane and the arrowhead points at the shear direction.

Fig.11. Typical results of interlayer materials from laboratory direct shear test by MSM (the size of sample is 150 mm × 150 mm × 150 mm) on the interlayer material from testing tunnel No.62 with the initial degree of saturation between 17.9% and 48.7%.

Fig.12. Shear stress versus normal stress of laboratory direct shear test on interlayer material by MSM

Fig.13. Typical results of interlayer materials from laboratory direct shear test by SSM (the size of sample is 150 mm × 150 mm × 150 mm) on the interlayer material from testing tunnel No.62 at an initial degree of saturation $S_r = 33.1\%$.

Fig.14. Typical results of shear creep test on interlayer material from testing tunnel No.41 at an initial degree of saturation $S_r = 24.2\%$ under an initial normal stress $\sigma_n = 0.49$ MPa.

Fig.15. Strength parameters versus clay fraction; (a) friction angle, (b) cohesion.

Fig.16. Strength parameters versus initial degree of saturation; (a) friction angle, (b) cohesion.

TABLE 1—Physical properties of interlayer material (ECIDI 2006)

No	Clay fraction ($< 2 \mu\text{m}$ %)	w (%)	ρ (Mg/m^3)		G_s	e	S_r (%)	w_L (%)	w_P (%)
			wet	dry					
1	10.1	13.6	2.19	1.93	2.95	0.529	76.1	24.7	13.9
2	7.1	13.4	2.27	1.98	2.88	0.455	84.9	24.9	14.7
3	4.8	13.0	2.13	1.86	2.78	0.494	73.0	27.8	16.5
4	13.8	14.8	2.25	1.96	2.83	0.447	93.5	24.7	14.1
5	6.3	8.0	2.35	2.17	2.81	0.292	76.6	-	-

- Values not available. Clay corresponds to the particle whose diameter is smaller than 0.005 mm according to the China National Standards GB/T 50145-2007.

TABLE 2—Initial parameters of the samples and strength parameters for the in-situ tests

No.	Clay fraction ($< 5\mu\text{m}$ %)	S_r (%)	c (MPa)	φ ($^\circ$)
1	13.0	99.5	0.02	14.0
1	11.0	76.6	0.13	21.3
2	8.5	96.6	0.07	21.3
2	0	73.0	0.42	38.0
3	10.5	79.6	0.11	18.8
3	12.0	85.6	0.03	21.3
4	12.5	93.5	0.06	14.0
5	0	76.6	0.05	25.6

TABLE 3—Initial parameters of the samples and strength parameters for the laboratory tests by MSM

No.	Clay fraction ($< 5\mu\text{m}$ %)	S_r (%)	Failure envelope		c^* (MPa)	φ^* ($^\circ$)
			σ_n (MPa)	τ_p (MPa)		
1	5.7	27.5	2.08	1.74	0.2	36.5
1	9.7	24.2	2.10	1.86	0.2	38.3
4	10.0	38.6	2.33	2.07	0.2	38.7
4	5.2	17.9	3.17	2.09	0.2	30.8
4	9.5	41.8	4.10	1.73	0.2	20.5
4	7.7	25.3	4.20	2.33	0.2	26.9
4	7.0	32.1	5.26	3.28	0.2	30.4
4	15.1	32.5	5.30	2.80	0.2	26.1
4	13.5	48.7	5.41	4.09	0.2	35.7

c^* is assumed as 0.2 MPa and φ^* is back calculated using the Mohr-Coulomb strength criterion.

TABLE 4—Initial parameters of the samples and strength parameters for the laboratory tests by SSM

No.	Clay fraction (< 5 μ m %)	S_r (%)	c (MPa)	ϕ (°)
4	7.3	33.1	0.39	28.6
1	5.2	33.3	0	20.8
4	8.7	38.4	0	29.8
4	7.0	32.2	0.051	27.1
4	6.3	32.2	0.011	23.6
4	10.4	29.6	0.079	23.4
4	7.7	39.5	0	28.9

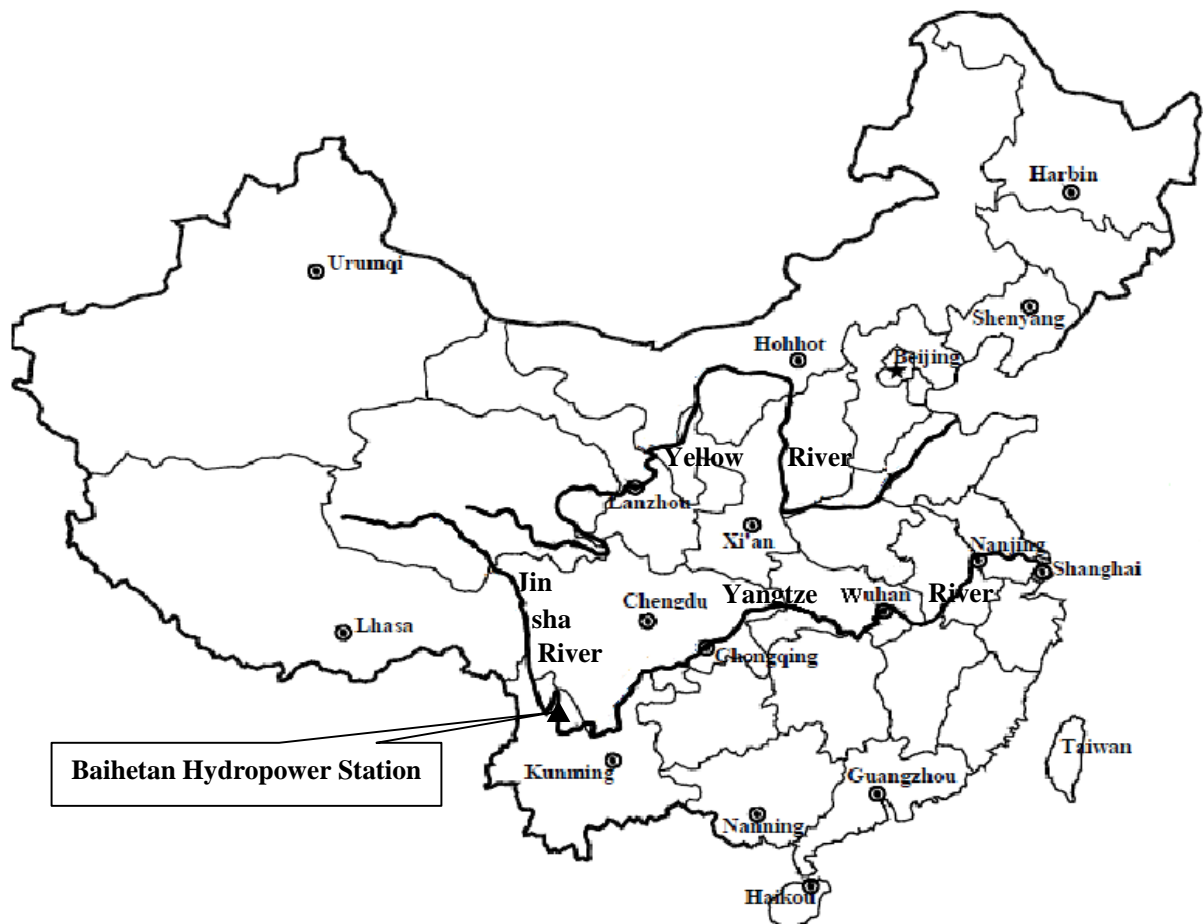


Fig.1. Location of Baihetan Hydropower Station.



Fig.2. *Interlayer staggered zone in testing tunnel No.62.*

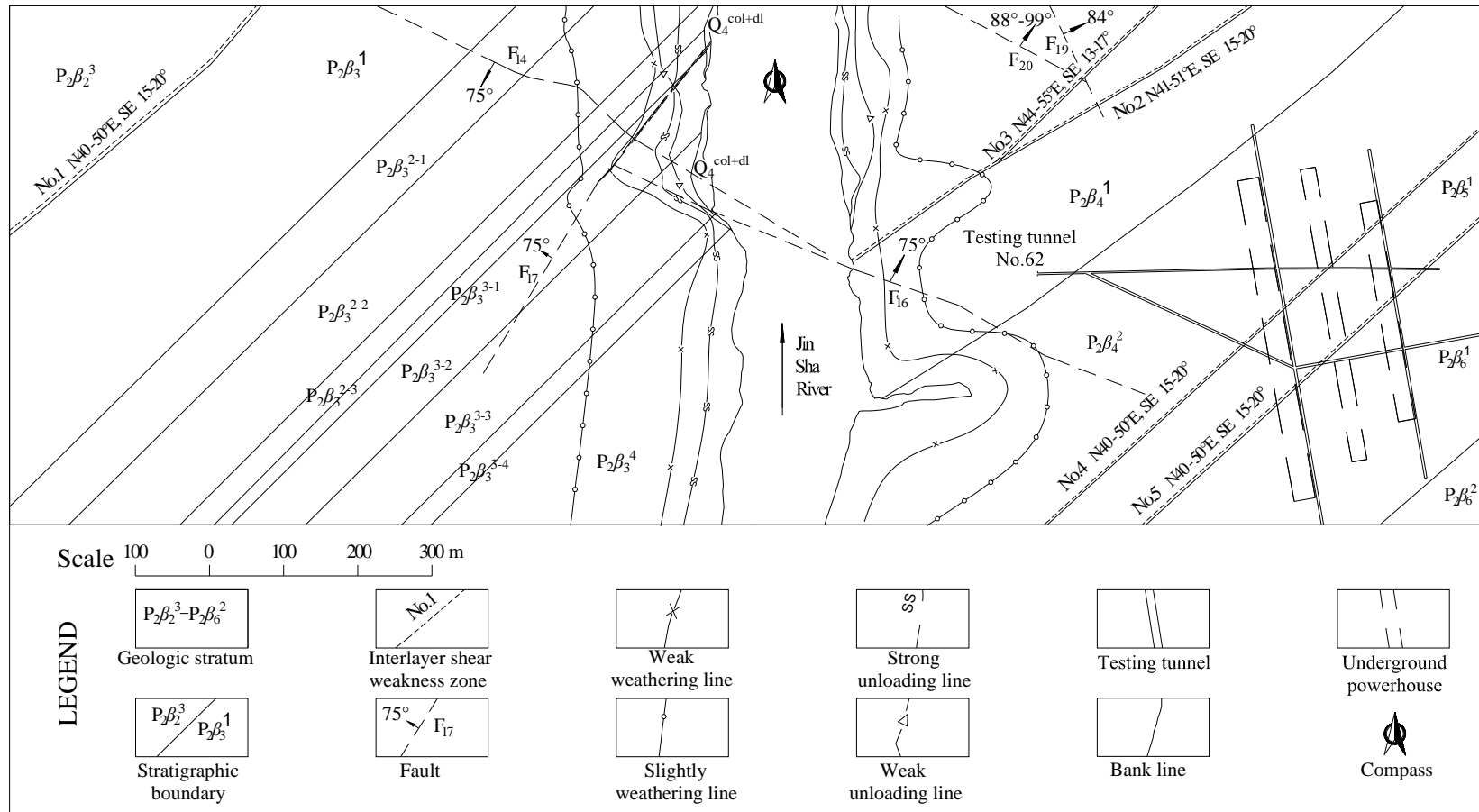


Fig.3. Geological map at an elevation of 624 m where testing tunnel No.62 is located (1) $P_2\beta_2^3$: Aphanitic basalt, amygdaloidal basalt, breccia lava; (2) $P_2\beta_3^1$: Aphanitic basalt, breccia lava with oblique basalt and amygdaloidal basalt with oblique basalt; (3) $P_2\beta_3^{2-1}$: Amygdaloidal basalt; (4) $P_2\beta_3^{2-2}$: Columnar jointed basalt; (5) $P_2\beta_3^{2-3}$: Breccia lava; (6) $P_2\beta_3^3$: Columnar jointed basalt; (7) $P_2\beta_3^4$: Amygdaloidal basalt, aphanitic basalt and breccia lava; (8) $P_2\beta_3^5$: Oblique basalt, breccia lava; (9) $P_2\beta_4^1$: Columnar jointed basalt, amygdaloidal basalt, breccia lava and microcrystalline basalt; (10) $P_2\beta_4^2$: Amygdaloidal basalt, breccia lava; (11) $P_2\beta_5^1$: Aphanitic basalt and amygdaloidal basalt; (12) $P_2\beta_6^1$: Columnar jointed basalt and breccia lava; (13) $P_2\beta_6^2$: Aphanitic basalt and breccia lava; (14) Q_4^{col+dl} : Quaternary unconsolidated deposits.

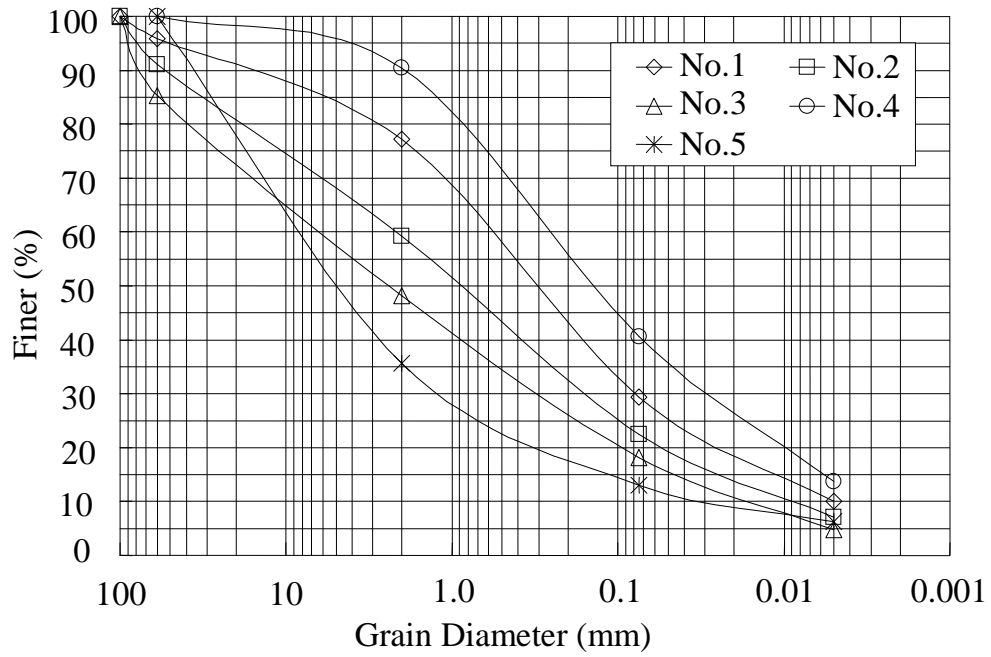


Fig. 4. Grain size distribution of interlayer material.

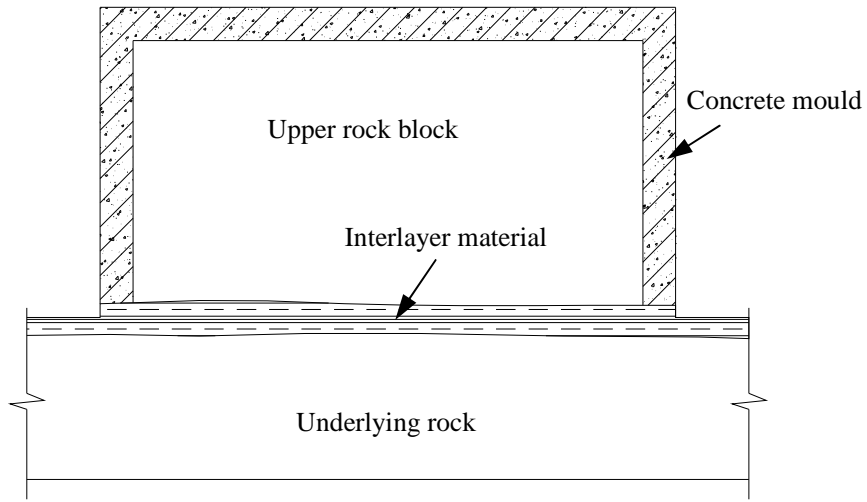


Fig. 5. The sketch of sample for the in-situ direct shear test

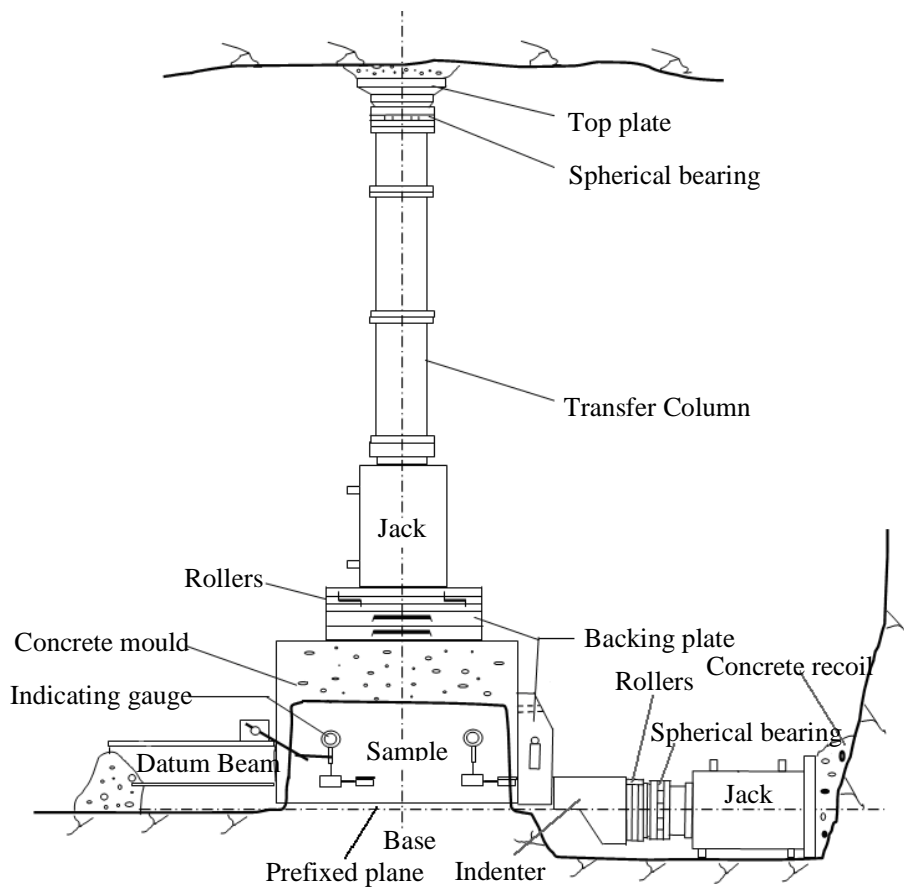


Fig.6. Schematic layout of in-situ direct shear test.

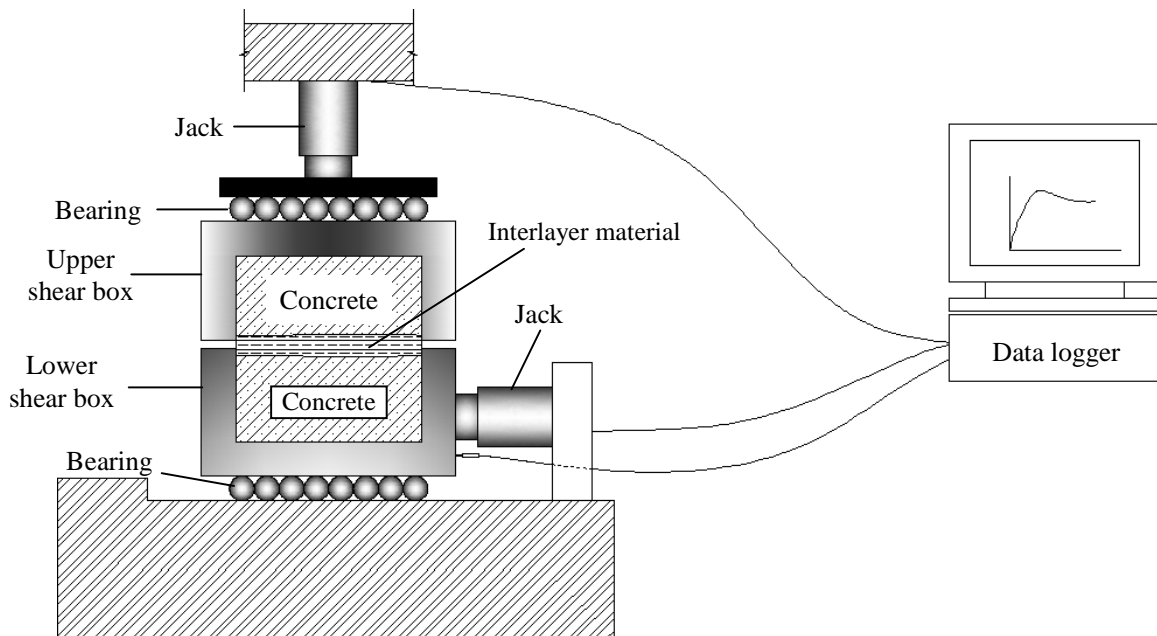


Fig.7. Schematic diagram of RMT150C.

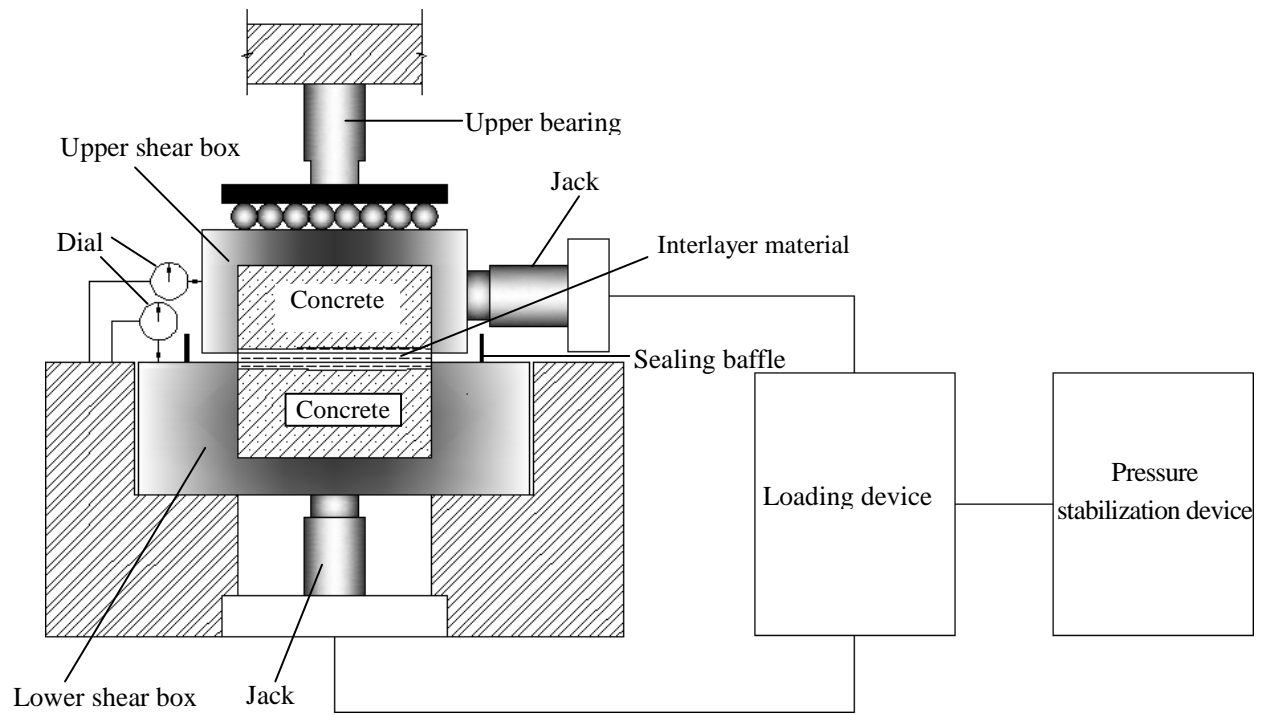
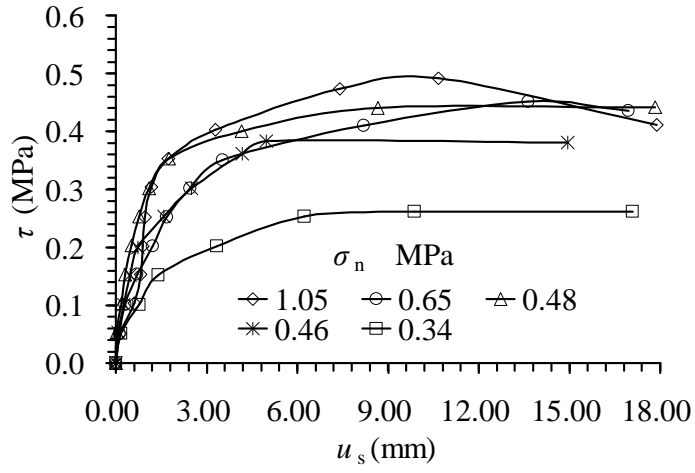
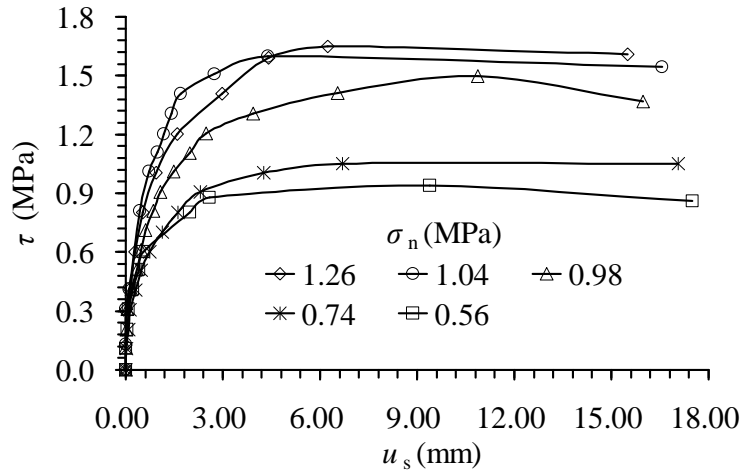


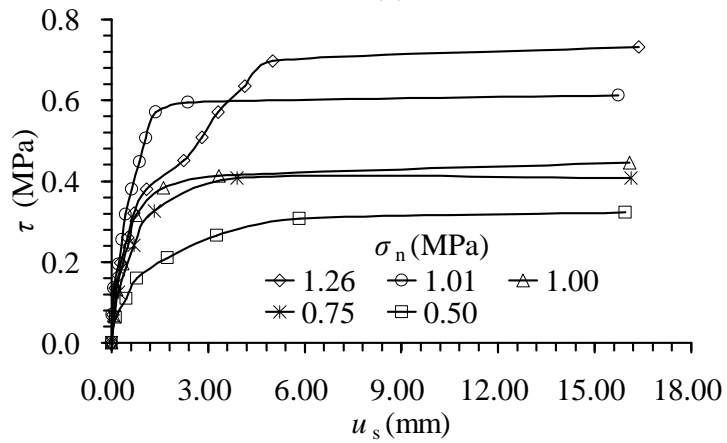
Fig.8. Schematic diagram of JQ-200.



(a)



(b)



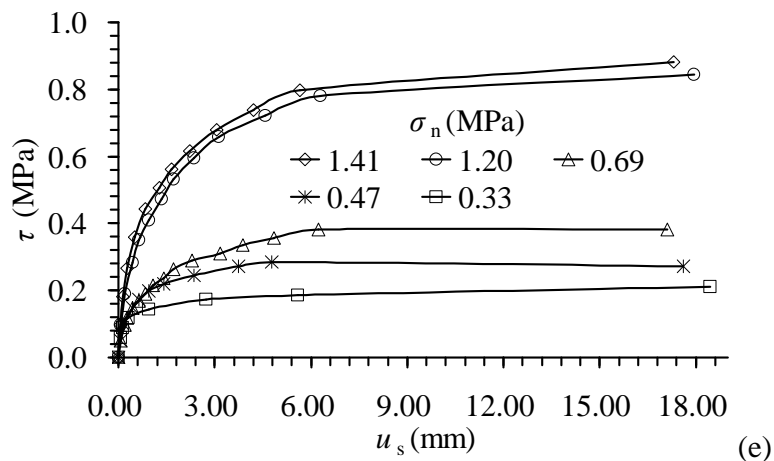
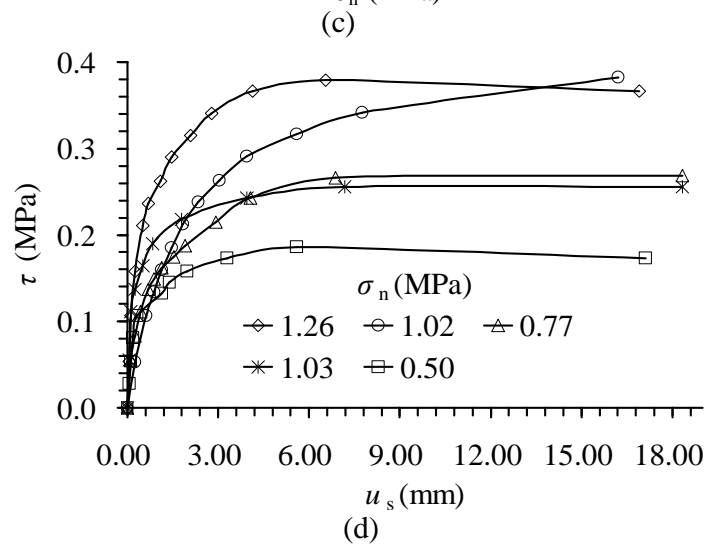
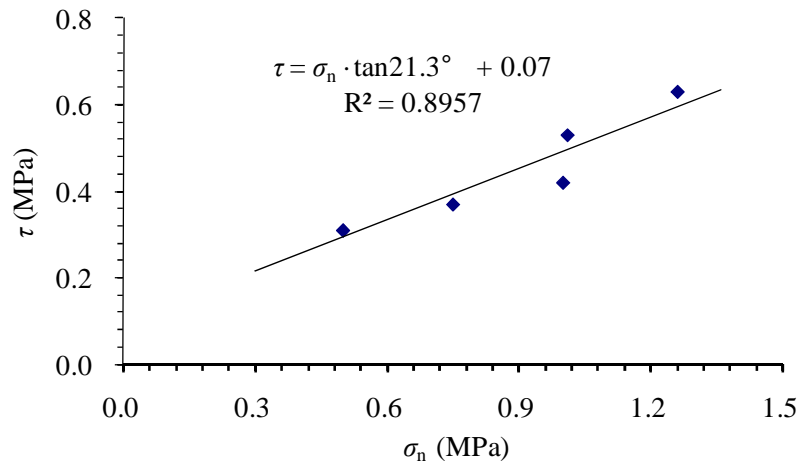


Fig.9. Typical results of interlayer materials of in-situ direct shear tests where the size of sample is 500 mm × 500 mm × 350 mm: from the interlayer staggered zone No.1 at an initial degree of saturation $S_r = 76.6\%$ (a), from the interlayer staggered zone No.2 at an initial $S_r = 73.0\%$ (b), from the interlayer staggered zone No.3 at an initial $S_r = 96.6\%$ (c), from the interlayer

staggered zone No.4 at an initial $S_r = 93.5\%$ (d), and from the interlayer staggered zone No.5 at an initial $S_r = 76.6\%$ (e).

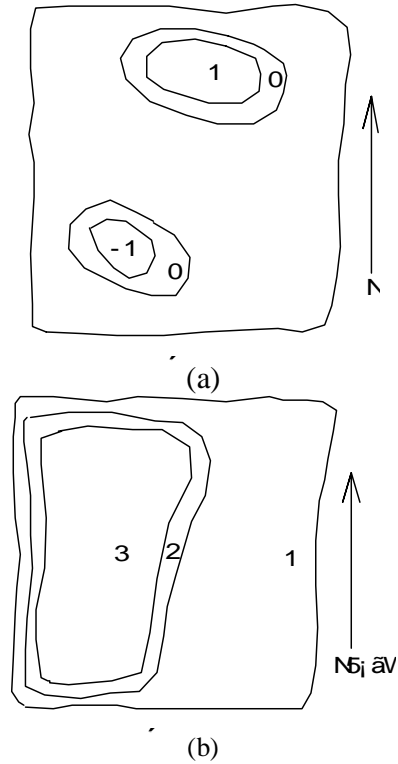
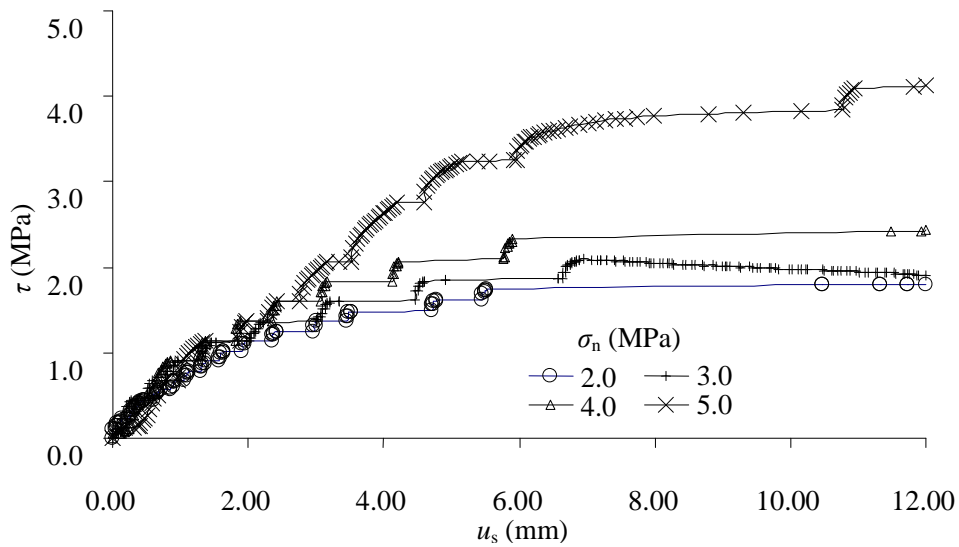


Fig.10. The shear surfaces of samples for a set of in-situ shear tests in zone 4: (a) normal shear surface, (b) irregular shear surface. The unit of numbers is centimeter, the negative number means the region is below the prefixed shear plane and the arrowhead points at the shear direction.



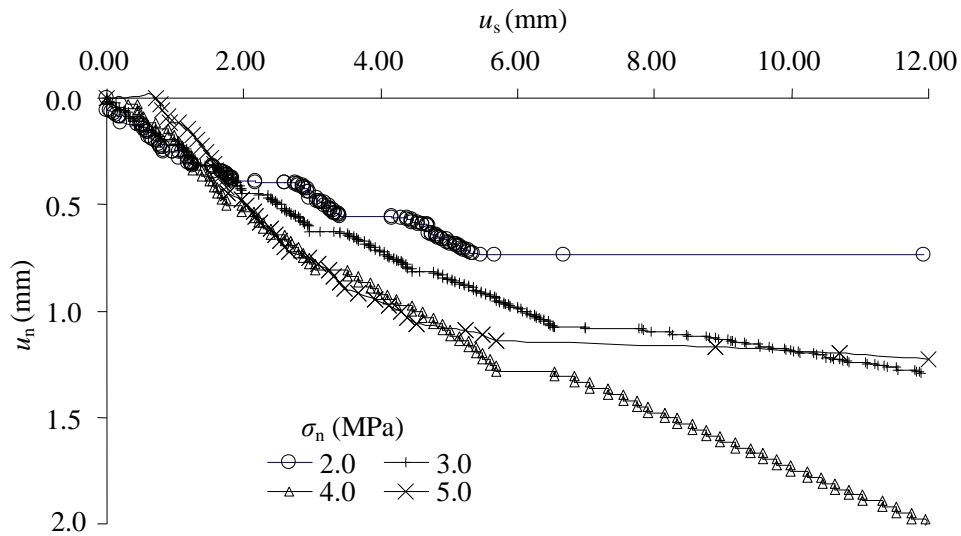


Fig.11. Typical results of interlayer materials from laboratory direct shear test by MSM (the size of sample is 150 mm × 150 mm × 150 mm) on the interlayer material from testing tunnel No.62 with the initial degree of saturation between 17.9% and 48.7%.

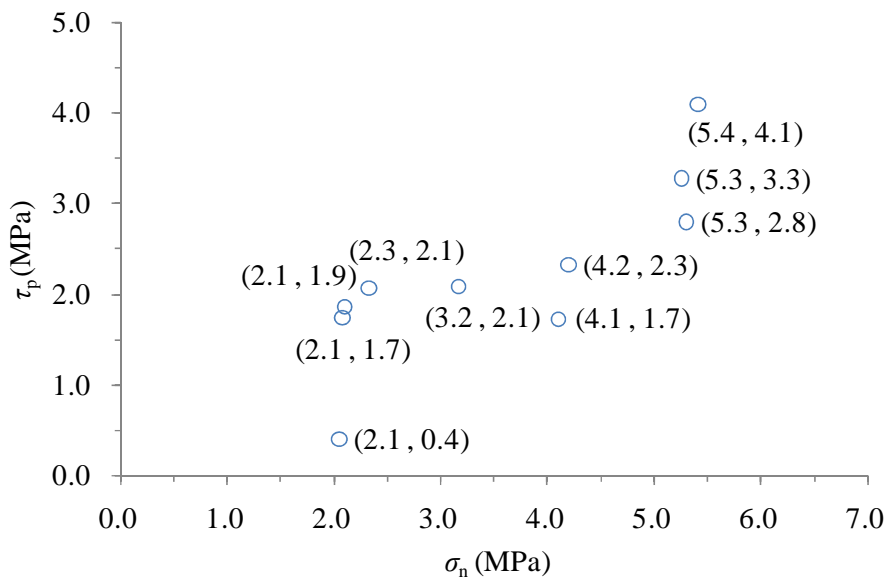


Fig.12. Shear stress versus normal stress of laboratory direct shear test on interlayer material by MSM.

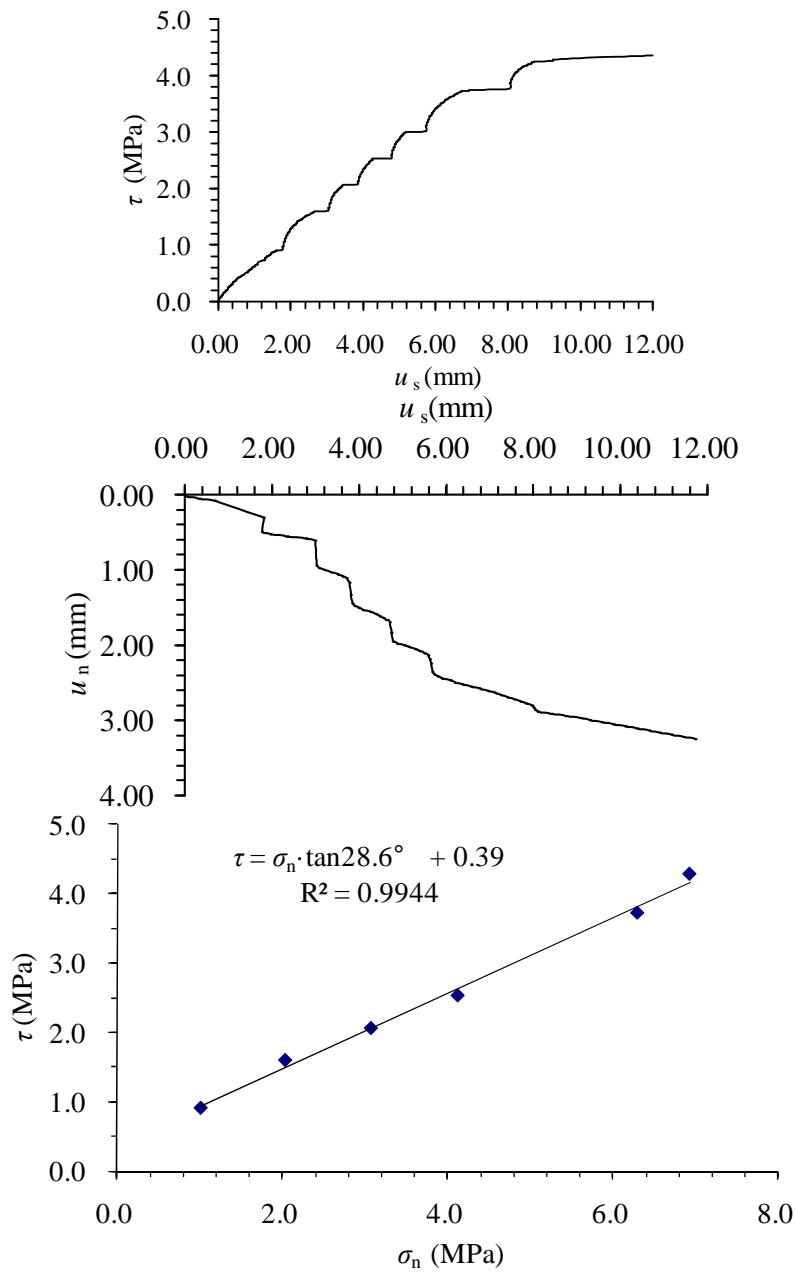


Fig.13. Typical results of interlayer materials from laboratory direct shear test by SSM (the size of sample is 150 mm × 150 mm × 150 mm) on the interlayer material from testing tunnel No.62 at an initial degree of saturation $S_r = 33.1\%$.

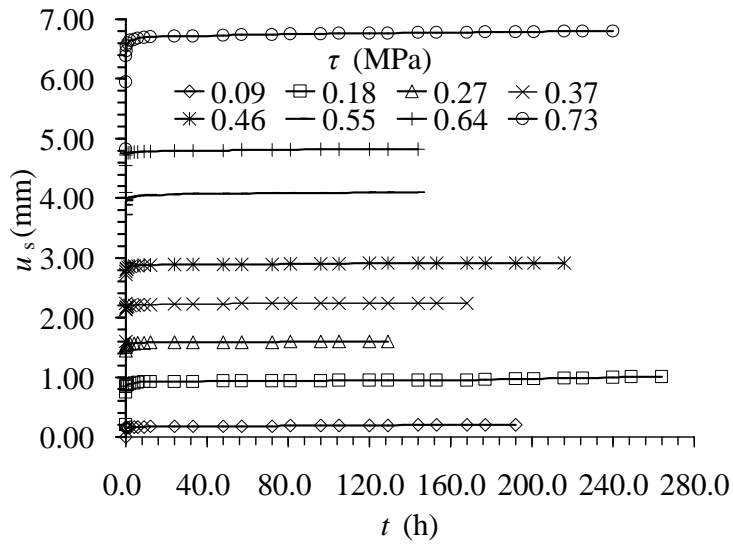
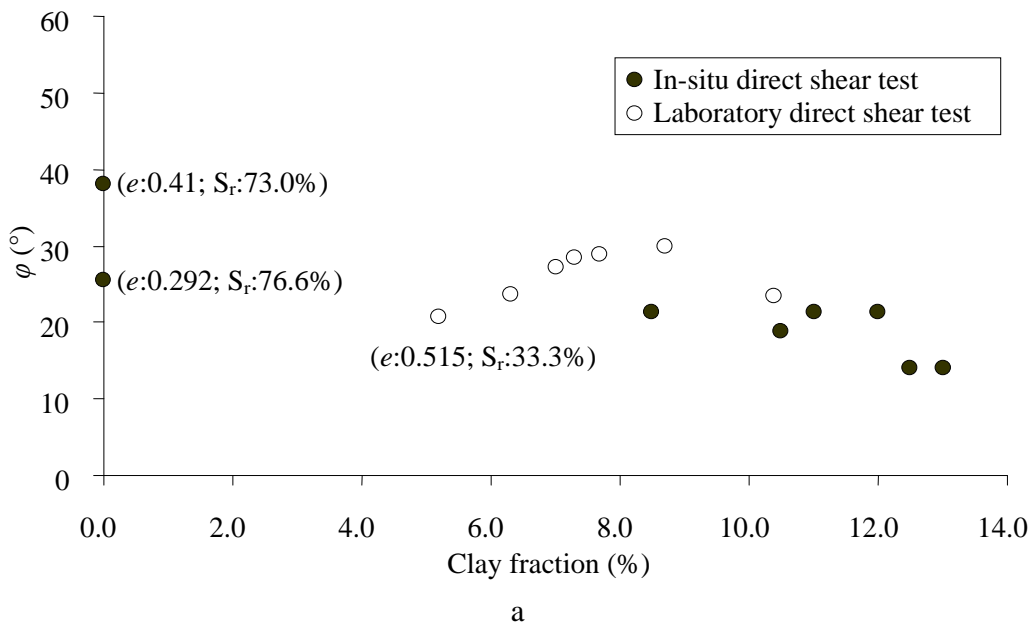


Fig.14. Typical results of shear creep test on interlayer material from testing tunnel No.4 at an initial degree of saturation $S_r = 24.2\%$ under an initial normal stress $\sigma_n = 0.49$ MPa.



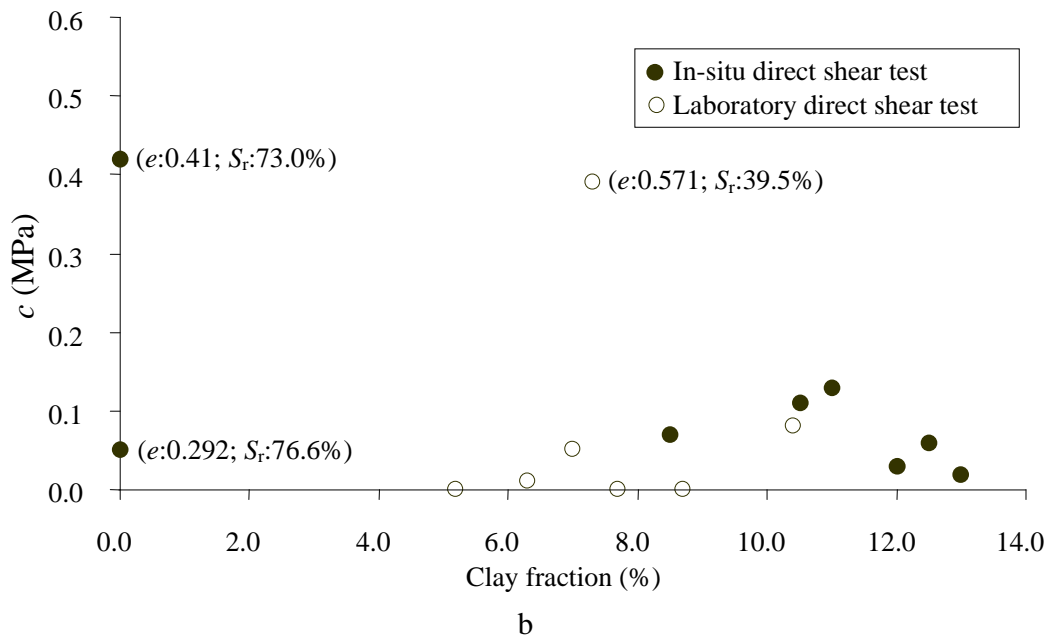
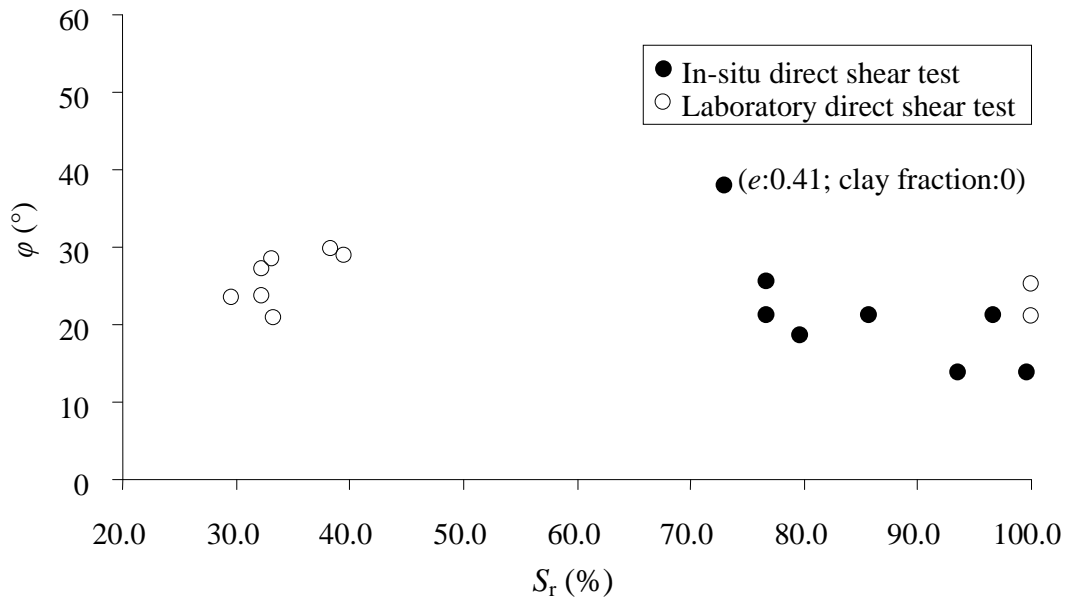
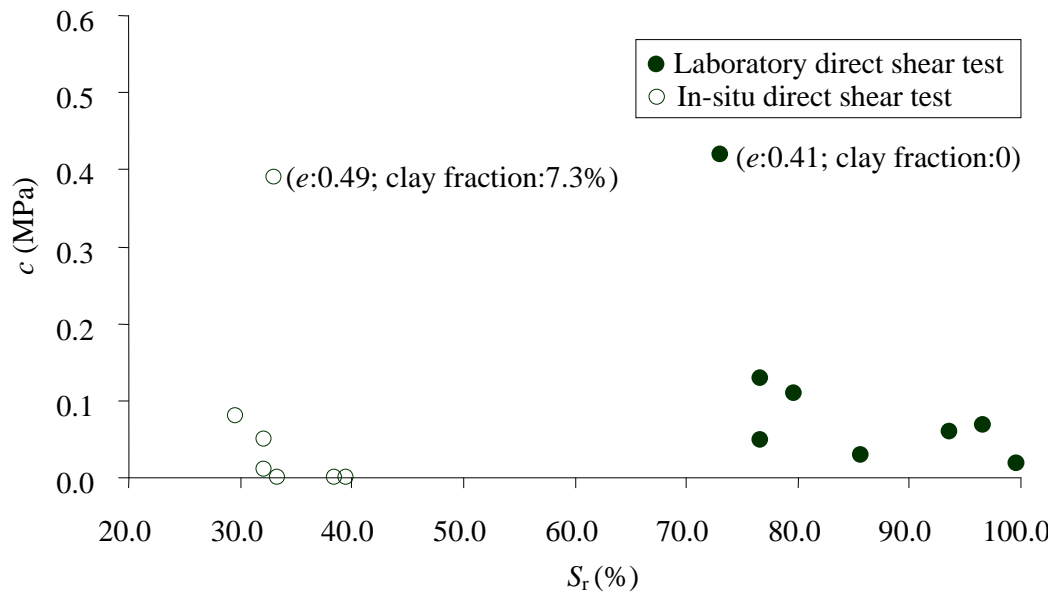


Fig.15. Strength parameters versus clay fraction; (a) friction angle, (b) cohesion.



a



b

Fig.16. Strength parameters versus initial degree of saturation; (a) friction angle, (b) cohesion.